Available online at www.sciencedirect.com

SCIENCE DIRECT®

Vision Research 45 (2005) 147–151

Vision Research

www.elsevier.com/locate/visres

Two realms of dark adaptation

M.L. Firsov, A.V. Kolesnikov, E.Yu. Golobokova, V.I. Govardovskii *

Institute for Evolutionary Physiology and Biochemistry, Russian Academy of Sciences, 44 Thorez Prospect, 194223 St. Petersburg, Russia

Received 7 June 2004; received in revised form 6 August 2004

Abstract

The recovery of rod responsiveness after saturating flashes is greatly retarded above a certain critical level of rhodopsin bleaching (~0.1%). A mathematical description of the process of turn-off of the phototransduction cascade allows attributing different phases of the recovery to specific products of rhodopsin photolysis. The fast phase is determined by quenching of metarhodopsin II and activated transducin. The slow phase is controlled by decay of partially inactivated (phosphorylated and arrestin-bound) metarhodopsins, and by regeneration of rhodopsin. The transition between the two regimes of adaptation is rather abrupt, occurring within a few-fold range of stimulus intensity. This marks the border between reversal of light adaptation and dark adaptation, as it is commonly defined.

Keywords: Rod; Dark adaptation; Rhodopsin; Metarhodopsin

1. Introduction

In a broad sense, the process of adjustment of photoreceptor sensitivity to ambient illumination can be called light adaptation while the inverse process of restoration of the pre-stimulus state—dark adaptation. Thus one may ask why the forward and backward reactions are usually treated separately, and different mechanisms are sought for them. Light adaptation is considered a result of a complex interplay of reactions that quickly activate and then quench the phototransduction cascade. Dark adaptation is usually considered a result of slower quenching reactions dependent on the decay of the products of rhodopsin photolysis and regeneration of "dark" rhodopsin (reviews: Fain, Matthews, Cornwall, & Koutalos, 2001; Lamb & Pugh, 2004; Pugh & Lamb, 2000, chapter 5).

Here, we show that the recovery of a rod from a light-adapted state occurs in two distinct temporal phases, depending on the level of rhodopsin bleaching. A simple mathematical description of the process of turn-off of the phototransduction cascade allows attributing different phases of the recovery to specific products of rhodopsin photolysis. The fast phase is determined by rapid quenching of metarhodopsin II (MII) that primarily activates the cascade, and by turn-off of activated transducin. The slow phase is mostly controlled by thermal decay of partially inactivated (phosphorylated and arrestin-bound) long-living intermediates (metarhodopsins), and by regeneration of rhodopsin. The transition between the two phases is determined by the degree of rhodopsin bleaching and is rather sharp. This justifies apposing dark adaptation to the reversal of light adaptation.

2. Experimental procedure

Photoresponses were recorded from isolated solitary rods of the frog *Rana ridibunda* by suction pipette technique, as described by Firsov, Donner, and Govardovskii (2002). Cells were stimulated with flashes of

* Corresponding author. Tel.: +7 812 550 4989; fax: +7 812 552 3012.

E-mail address: vgov@mailbox.alkor.ru (V.I. Govardovskii).

0042-6989/$ - see front matter © 2004 Elsevier Ltd. All rights reserved.
doi:10.1016/j.visres.2004.08.005

525-nm light from a light-emitting diode (#110104 from Marl International Ltd., UK). Stimulus intensity was controlled by neutral filters, diode current, and the flash duration. Absolute intensity calibration in terms of the number of rhodopsin molecules activated per rod per flash (R*) was achieved using the statistics of the responses to weak (2–4 R*) stimuli (Baylor, Lamb, & Yau, 1979). Every cell was also videorecorded to determine its dimensions and calculate the cell's light collecting area. It allowed specifying the stimulus intensity in terms of photons per squared micron or fractional bleaches, to account for variations in the outer segment volume among cells. The system of differential equations describing the kinetic scheme of quenching the phototransduction cascade was solved numerically using MathCad 2001*i* Professional (MathSoft Engineering & Education, Inc., Cambridge, MA).

3. Results

Current flowing through the light-sensitive channels of the rod outer segment is controlled by the concentration of the intracellular messenger, cGMP. cGMP concentration is set by a balance between its synthesis by guanylate cyclase and hydrolysis by light-activated phosphodiesterase (PDE). In light, accelerated hydrolysis results in [cGMP] decrease and the closure of the channels. Subsequent quenching of the hydrolytic activity leads to [cGMP] recovery, and restoration of the circulating current. Both the synthesis and light-induced hydrolysis of cGMP are under a strong negative feedback control that operates via the cytoplasmic concentration of Ca^{2+} ions (recent reviews: Burns & Baylor, 2001; Burns & Lamb, 2003, chapter 16; Pugh & Lamb, 2000, chapter 5). Bright saturating flashes result in complete closure of all channels, so the rod stays in saturation for progressively longer times with increasing light intensities (Fig. 1(A)). Recovery from saturation restores the rod's responsiveness thus manifesting the process of dark adaptation.

Remarkably, dark adaptation proceeds in two distinct phases. At low and moderate flash intensities, time in saturation smoothly increases with increasing stimulus strength, showing an approximately linear dependence on the log(Intensity) (*I*, expressed here as photons μm^{-2}) (Fig. 1(B), solid line; cf. Nikonov, Engheta, & Pugh, 1998; Pepperberg et al., 1992). Above a certain critical brightness, however, dark adaptation becomes drastically retarded, so the t_{sat} vs. log(*I*) plot makes a sharp bend (dashed line in Fig. 1(B)). Obviously, the transition between the two branches of the curve, occurring at ~0.1% bleach, corresponds to a transition between (at least) two processes that underlie dark adaptation.

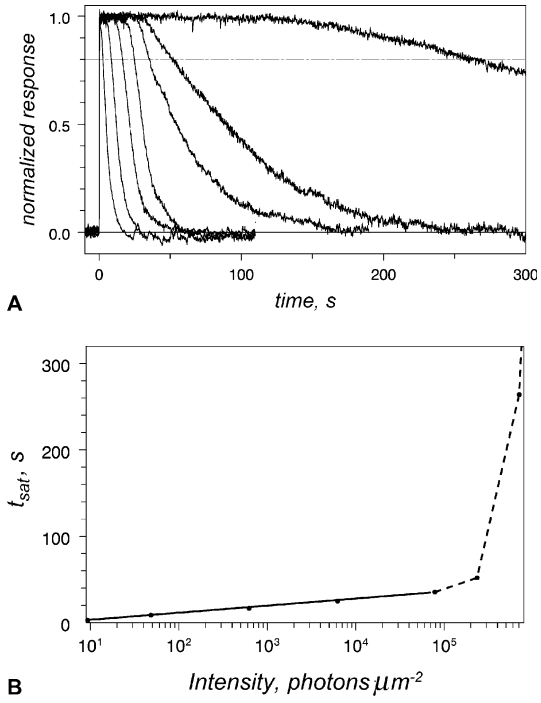

Fig. 1. Two-phase recovery from saturation in a frog rod: (A) sample recordings of the rod response to saturating flashes of increasing intensity. Flash intensities 2×10^2, 1.3×10^3, 1.65×10^4, 1.65×10^5, 2.1×10^6, 6.2×10^6, 1.9×10^7 R*, rod's light collecting area 26.6 μm^2; (B) time in saturation vs. intensity function. Time in saturation is defined as the time until recovery of 20% circulating current marked with the dot-dashed line in (A). Solid line is the linear fit to t_{sat} vs. ln(Intensity) for first five points, yielding the Pepperberg time constant of 3.5 s.

By examining the t_{sat} vs. *I* plot, one can characterize the time course of quenching of the light-induced PDE activity. Assuming that the period of saturation, when all light-sensitive channels are closed, is long enough to completely activate the Ca^{2+}-feedback, a fixed level of partial recovery of the circulating current corresponds to a fixed level of recovery of [cGMP]. This in turn means that the post-flash PDE activity *P*(*t*) produced by a flash of intensity *I* fell from its maximum value down to a certain fixed criterion level set by fully activated guanyl cyclase:

$$P(t_{sat}) = I \cdot p(t_{sat}) = c \tag{1a}$$

or

$$p(t_{sat}) = c\frac{1}{I} \tag{1b}$$

Here *p*(*t*) is the wave of PDE activity elicited by 1 photon μm^{-2} flash, and *c* = const. is the criterion level. In other words, fractional activity of PDE at a certain time *t* is inversely proportional to the intensity of the flash that results in saturation time $t_{sat} = t$. Hence, plotting inverse stimulus intensity vs. time in saturation, one gets the time course of PDE quenching. The procedure is

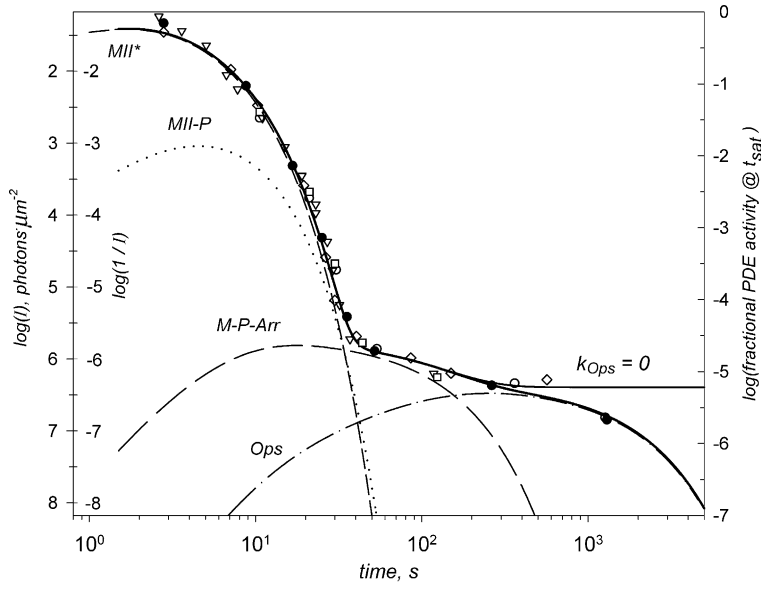

Fig. 2. Time course of quenching of flash-induced PDE activity. Symbols, data from five cells processed accordingly to Eq. (1b). Data from the cell in Fig. 1 are marked by solid circles. Thick solid line, theoretical prediction based on the kinetic scheme of Fig. 3 using the parameters from Table 1. Dashed and dotted lines show contribution of each component of the kinetic scheme to total PDE activity. Thin solid line, no rhodopsin regeneration.

illustrated in Fig. 2 that can merely be considered as Fig. 1(B) rotated by 90° clockwise to swap x- and y-axes. It is also re-plotted on log–log scale to encompass a wide range of times and intensities. Notice that the intensity (left labels on left y-axis) is now increasing downward (which on log scale is obviously equivalent to plotting $1/I$ term of Eq. (1b) increasing upward, as shown by right labels on left axis). Thus the solid circles in Fig. 2, when referred to the right labels, give the $1/I$ vs. t_{sat} function for the cell shown in Fig. 1, that is, $p(t)$ scaled by yet unknown c.

On the other hand, the time course of flash-induced PDE activity, $p(t)$, can be predicted based on certain assumptions about the processes of PDE activation and turn-off. A generalized kinetic scheme of the quenching of activated rhodopsin and PDE is shown in Fig. 3. The rate of activation of transducin by photoactivated rhodopsin (MII*) is greatly reduced by its phosphorylation (formation of MII–P), and then by arrestin binding: forming M–P–Arr. Here M denotes all metarhodopsin species (MI, MII and MIII) that may contribute to transducin activation (Kolesnikov, Golobokova, & Govardovskii, 2003; Leibrock & Lamb, 1997; Leibrock, Reuter, & Lamb, 1994, 1998). Finally, M decays to all-*trans* retinal and opsin (Ops) that subsequently regenerates to rhodopsin (Rh) by binding 11-*cis* retinal. The first-order rate constants of corresponding reactions are k_{MII}, k_{MIIp}, k_{MA} and k_{Ops} (s^{-1}), and fractional (with respect to MII*) catalytic activities of the products, a_{MII}, a_{MIIp}, a_{MA}, a_{Ops} and a_{Rh} (Fig. 3). The kinetic scheme, combined with the rate constant of transducin/PDE inactivation k_{PDE}, is described by a system

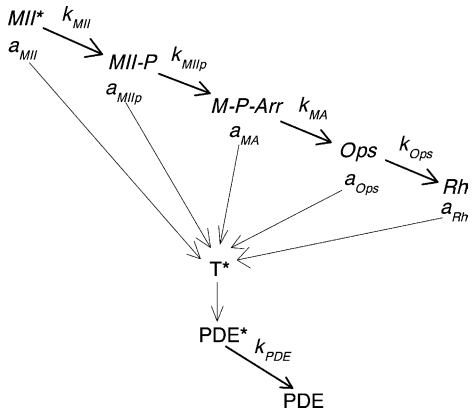

Fig. 3. A kinetic scheme of quenching the cGMP-hydrolytic activity of the phototransduction cascade. Asterisks denote fully activated molecular forms of MII, T, and PDE. Explanation in the text.

of five first-order linear differential equations. Its solution gives the time course of the catalytic activity of phosphodiesterase after unit intensity flash ($p(t)$ in Eqs. 1a, b)) that is plotted in Fig. 2 against the right y-axis with thick solid line. Mutual positioning of the left and right axes depends on the criterion level c; changes in c result in a vertical shift of the theoretical curve with respect to experimental points. Thus c-value was initially chosen to fit experimental data for the cell from Fig. 1. Raw sets of data for four other cells (empty symbols in Fig. 2), when plotted against the left axis, are displaced with respect to each other yet follow a common trend. They can be brought to the same function by simply shifting each set vertically by no more than 0.08 log units which can be interpreted as <20%

variations in the criterion level (maximum guanyl cyclase activity) among the cells.

Fig. 2 shows that the kinetic scheme provides a good fit to experimental data. The decline of the flash-induced PDE activity indeed follows a two-phase time course, with a fast phase dominant during ca. 30 s and followed by a much slower component that lasts, in the frog rods, for >1 h. Dashed and dotted lines in Fig. 2 show partial PDE activities elicited by individual states of photolyzed rhodopsin. It is obvious that a substantial part of the slow phase, between 30 s and 5 min postbleach, is dominated by decaying metarhodopsins. The rest of the slow phase is controlled by the formation and decay of "naked" opsin that arises from M and then binds 11-*cis* retinal to regenerate rhodopsin.

Parameters of the fit are given in Table 1. They have roughly been estimated from our own experimental data and the data available in the literature, and further refined by trials. Quality of the fit was judged by eye. Thus, initial k_{PDE} value was taken as the inverse slope of the Pepperberg plot at low intensities (solid line in Fig. 1). k_{MA} is known from microspectrophotometry measurements (Kolesnikov et al., 2003). The rate constant of rhodopsin regeneration k_{Ops} is within the range reported for intact frog eye ($\sim 7 \times 10^{-4}$ s^{-1} at 20 °C, Donner & Reuter, 1976, chapter 8) and isolated retina (2×10^{-3} s^{-1}, Azuma, Azuma, & Sickel, 1977). Since it is not certain that rhodopsin regeneration proceeds in isolated rods used in our experiments, the prediction for $k_{Ops} = 0$ is also shown in Fig. 2 with a thin solid line.

Quality of the fit is grossly insensitive to the values of k_{MIIp} and a_{MIIp} that characterize the properties of phosphorylated but arrestin-free MII (MII–P). An increase in k_{MIIp} can, to a certain extent, be compensated by an increase in a_{MIIp}, and v.v. However, setting $a_{MIIp} < 0.002$ or $a_{MIIp} > 0.05$ leads to a perceptibly poorer fit to the fast phase that determines the range of probable a_{MIIp} values. Likewise, the range of k_{MIIp} providing a good fit lies between 0.25 and 0.8 s^{-1}. Clearly, a more detailed study of the recovery between ~10 and 30 s is necessary to accurately determine the lifetime and activity of MII–P.

As for fractional activities of other forms of partially quenched rhodopsin, it is not easy to confront the values from Table 1 with biochemical data. In vitro studies of this sort have not been able to measure the basic reference value, the full activity of MII*, that would satisfy physiological demands. Only a few, specially dedicated experiments have demonstrated the activity that could be reconciled with the physiological sensitivity of a dark-adapted rod (for review see Leskov et al., 2000), yet most of them did not deal with any quenched form. Thus, the main independent source of data for comparison is physiological experiments. The value of a_{MA}, fractional activity of phosphorylated and arrestin-bound metarhodopsin(s), has been estimated for toad rods by Leibrock et al. (1994, 1998) who measured the desensitizing effect of ~0.02–3% rhodopsin bleaching and expressed it in terms of "equivalent background". Total activity of quenched metarhodopsins, that is, their ability to generate a "photon-like" signal and steady desensitization, was found to correspond to $\sim 5 \times 10^{-6}$–10^{-5} activity of MII*. This is in a close agreement with the value in Table 1. Similarly, the activity of "naked" opsin has been determined from its desensitizing effect on strongly bleached salamander rods (Cornwall & Fain, 1994). Again, the result, $\sim 10^{-6}$, is in a good agreement with the value estimated from Fig. 2. Remarkably, the most careful biochemical estimate of this activity by Melia, Cowan, Angleson, and Wensel (1997) yielded almost exactly the number shown in the Table 1 (2×10^{-6}). As for the activity of "dark" rhodopsin (a_{Rh}), it is clearly below the lower margin of Fig. 2 and is irrelevant here.

Non-uniform time course of rod recovery from saturating flashes has been noticed before in studies on both amphibian (Nikonov et al., 1998) and mammalian rods (Burns, Mendez, Chen, & Baylor, 2002; Calvert et al., 2001; Makino et al., 2004), including humans (Pepperberg, Birch, Hofmann, & Hood, 1996). Deviations from a straight Pepperberg plot have been interpreted as interference from a slower recovery process whose possible nature has been discussed (see e.g. Lyubarsky & Pugh, 1996; Pepperberg et al., 1996). However, all the studies have been confined to saturation times not exceeding a few seconds in mammals and 20 s in amphibians, well below the characteristic time of dark adaptation. Here we show that a realistic kinetic scheme of quenching of the phototransduction cascade that takes into account the fate and signaling activities of late products of rhodopsin photolysis provides a good explanation for the two-phase recovery of retinal rods from saturation after strong bleach. It justifies separating the process of restoration of the dark-adapted state into two realms. At relatively low intensities, the cell regains its sensitivity by using essentially the same fast mechanisms that quench single-photon responses (MII* phosphorylation and arrestin binding, plus Ca^{2+}-feedback).

Table 1
First-order decay rate constants k (s^{-1}) and fractional activities (a) of rhodopsin intermediates as defined in Fig. 3

k_{MII}	k_{MIIp}	k_{MA}	k_{Ops}	k_{PDE}	a_{MII}	a_{MIIp}	a_{MA}	a_{Ops}	a_{Rh}
1.0	0.28	1.2×10^{-2}	8×10^{-4}	0.33	1	0.012	9×10^{-6}	2.1×10^{-6}	–

This way of recovery can be called ''inverse light adaptation''. It operates within more than six decimal orders of stimulus strength, from single photons to $\sim 3 \times 10^6$ photons. At higher (>0.1%) bleaches, fast quenching is complete while the cell still stays in saturation, so the recovery time is now determined by a slow decay of accumulated long-living products with low catalytic activities (phosphorylated and arrestin-bound metarhodopsin(s) and free opsin). A big difference between life times and activities of short-living and long-living intermediates makes the transition between the two regimes of adaptation rather abrupt, occurring within few-fold range of stimulus intensity (Figs. 1, 2). The transition between the two phases marks the border between inverse light adaptation and dark adaptation, as it is commonly defined.

Acknowledgments

Authors are thankful to Prof. Tom Reuter for important comments on the MS, and to John Hopp for the help with the English text. The work is supported by the Russian Foundation for Basic Research grants # 03-04-49713 and 03-04-48603.

References

Azuma, K., Azuma, M., & Sickel, W. (1977). Regeneration of rhodopsin in frog rod outer segments. *Journal of Physiology (London), 271*, 747–759.

Baylor, D. A., Lamb, T. D., & Yau, K.-W. (1979). Responses of retinal rods to single photons. *Journal of Physiology (London), 288*, 613–634.

Burns, M., & Baylor, D. A. (2001). Activation, deactivation and adaptation in vertebrate photoreceptor cells. *Annual Reviews of Neuroscience, 24*, 779–805.

Burns, M. E., Mendez, A., Chen, J., & Baylor, D. A. (2002). Dynamics of cyclic GMP synthesis in retinal rods. *Neuron, 36*, 81–91.

Burns, M. E., & Lamb, T. D. (2003). Visual transduction by rod and cone photoreceptors. In L. M. Chalupa & L. S. Werner (Eds.), *The visual neurosciences* (pp. 215–233). Cambridge, MA: MIT Press.

Calvert, P. D., Govardovskii, V. I., Krasnoperova, N., Anderson, R. E., Lem, J., & Makino, C. L. (2001). Membrane protein diffusion sets the speed of rod phototransduction. *Nature, 411*, 90–94.

Cornwall, M. C., & Fain, G. L. (1994). Bleached pigment activates transduction in isolated rods of the salamander retina. *Journal of Physiology (London), 480*(Pt 2), 261–279.

Donner, K. O., & Reuter, T. (1976). Visual pigments and photoreceptor function. In L. Llinas & W. Precht (Eds.), *Frog neurobiology* (pp. 251–277). Berlin, Heidelberg: Springer.

Fain, G. L., Matthews, H. R., Cornwall, M. C., & Koutalos, Y. (2001). Adaptation in vertebrate photoreceptors. *Physiological Reviews, 8*, 117–151.

Firsov, M. L., Donner, K., & Govardovskii, V. I. (2002). pH and the dark events rate in toad rods: Test of a hypothesis on the molecular origin of photoreceptor noise. *Journal of Physiology (London), 539*(3), 837–846.

Kolesnikov, A. V., Golobokova, E. Yu., & Govardovskii, V. I. (2003). The identity of metarhodopsin III. *Visual Neuroscience, 20*, 249–265.

Lamb, T. D., & Pugh, E. N. Jr., (2004). Dark adaptation and the retinoid cycle of vision. *Progress in Retinal and Eye Research, 23*, 307–380.

Leibrock, C. S., & Lamb, T. D. (1997). Effect of hydroxylamine on photon-like events during dark adaptation in toad rod photoreceptors. *Journal of Physiology (London), 501*, 97–109.

Leibrock, C. S., Reuter, T., & Lamb, T. D. (1994). Dark adaptation of toad rod photoreceptors following small bleaches. *Vision Research, 34*, 2787–2800.

Leibrock, C. S., Reuter, T., & Lamb, T. D. (1998). Molecular basis of dark adaptation in rod photoreceptors. *Eye, 12*, 511–520.

Leskov, I. B., Klenchin, V. A., Handy, J. W., Whitlock, G. G., Govardovskii, V. I., Bownds, M. D., et al. (2000). The gain of rod phototransduction: Reconciliation of biochemical and electrophysiological measurements. *Neuron, 27*, 525–537.

Lyubarsky, A. L., & Pugh, E. N. Jr., (1996). Recovery phase of the murine rod photoresponse reconstructed from electroretinographic recordings. *The Journal of Neuroscience, 76*, 563–571.

Makino, C. L., Dodd, R. L., Burns, M. E., Roca, A., Simon, M. I., & Baylor, D. A. (2004). Recoverin regulates light-dependent phosphodiesterase activity in retinal rods. *Journal of General Physiology, 123*, 729–741.

Melia, T. J., Cowan, C. W., Angleson, J. K., & Wensel, T. G. (1997). A comparison of the efficiency of G-protein activation by ligand-free and light-activated forms of rhodopsin. *Biophysical Journal, 73*, 3182–3191.

Nikonov, S., Engheta, H., & Pugh, E. N. Jr. (1998). Kinetics of recovery of the dark-adapted salamander rod photoresponse. *Journal of General Physiology, 111*, 7–37.

Pepperberg, D. R., Cornwall, M. C., Kahlert, M., Hofmann, K. P., Jin, J., Jones, G. J., et al. (1992). Light-dependent delay in the falling phase of the retinal rod photoresponse. *Visual Neuroscience, 8*, 9–18.

Pepperberg, D. R., Birch, D. G., Hofmann, K. P., & Hood, D. C. (1996). Recovery kinetics of human rod phototransduction inferred from the two-branched a—wave saturation function. *Journal of the Optical Society of America A, 13*, 586–600.

Pugh, E. N., Jr., & Lamb, T. D. (2000). Phototransduction in vertebrate rods and cones: Molecular mechanisms of amplification, recovery and light adaptation. In D. G. Stavenga, W. J. deGrip, & E. N. Pugh (Eds.). *Handbook of biological physics* (vol. 3, pp. 183–255). Amsterdam: Elsevier Science BV.